HHS Public Access

Author manuscript

Biosens Bioelectron. Author manuscript; available in PMC 2018 March 15.

Published in final edited form as:

Biosens Bioelectron. 2017 March 15; 89(Pt 1): 201–211. doi:10.1016/j.bios.2016.03.044.

Nucleic acid-functionalized transition metal nanosheets for biosensing applications

Liuting Mo[a], **Juan Li**[a,b], **Qiaoling Liu**[a,*], **Liping Qiu**[a], and **Weihong Tan**[a,c,*]

[a]Molecular Sciences and Biomedicine Laboratory, State Key Laboratory for Chemo/Biosensing and Chemometrics, College of Chemistry and Chemical Engineering and College of Biology, Collaborative Innovation Center for Molecular Engineering and Theranostics, Hunan University, Changsha 410082, China.

[b]The Key Lab of Analysis and Detection Technology for Food Safety of the MOE and Fujian Province, State Key Laboratory of Photocatalysis on Energy and Environment, College of Chemistry, Fuzhou University, Fuzhou 350002, China.

[c]Department of Chemistry and Department of Physiology and Functional Genomics, Center for Research at the Bio/Nano Interface, UF Health Cancer Center, University of Florida, Gainesville, FL 32611-7200, USA Fax: (+1) 352-846-2410.

Abstract

In clinical diagnostics, as well as food and environmental safety practices, biosensors are powerful tools for monitoring biological or biochemical processes. Two-dimensional (2D) transition metal nanomaterials, including transition metal chalcogenides (TMCs) and transition metal oxides (TMOs), are receiving growing interest for their use in biosensing applications based on such unique properties as high surface area and fluorescence quenching abilities. Meanwhile, nucleic acid probes based on Watson-Crick base-pairing rules are also being widely applied in biosensing based on their excellent recognition capability. In particular, the emergence of functional nucleic acids in the 1980s, especially aptamers, has substantially extended the recognition capability of nucleic acids to various targets, ranging from small organic molecules and metal ions to proteins and cells. Based on π-π stacking interaction between transition metal nanosheets and nucleic acids, biosensing systems can be easily assembled. Therefore, the combination of 2D transition metal nanomaterials and nucleic acids brings intriguing opportunities in bioanalysis and biomedicine. In this review, we summarize recent advances of nucleic acid-functionalized transition metal nanosheets in biosensing applications. The structure and properties of 2D transition metal nanomaterials are first discussed, emphasizing the interaction between transition metal nanosheets and nucleic acids. Then, the applications of nucleic acid-functionalized transition metal nanosheet-based biosensors are discussed in the context of different signal transducing mechanisms, including optical and electrochemical approaches. Finally, we provide our perspectives on the current challenges and opportunities in this promising field.

[*]Correspondinding author. qlliu@iccas.ac.cn, tan@chem.ufl.edu.

Keywords

Transition metal nanomaterials; Nucleic acids; Aptamers; Biosensors; Nanosheets

1. Introduction

Two-dimensional (2D) transition metal nanomaterials, including transition metal chalcogenides (TMCs) and transition metal oxides (TMOs), which possess planar morphology and ultrathin thickness, have received growing interest in the fields of electronics (Lembke et al. 2015; Radisavljevic et al. 2011b), sensors (Li et al. 2012; Sarkar et al. 2015; Yang et al. 2013), catalysis (Voiry et al. 2013; Xie et al. 2013), and energy harvesting (Chhowalla et al. 2013; Sun et al. 2014b). Moreover, these 2D nanosheets provide outstanding biosensing performance owing to their unique physical, chemical and electronic properties (Pumera and Loo 2014; Xu et al. 2013). In particular, their unique structure and specific surface area favor high loading efficiency for biomolecules. Many transition metal nanosheets also possess intrinsic fluorescence quenching abilities (Goswami et al. 2013; Liu and Lu 2007; Sakai et al. 2005), which could be applied in fluorescence resonance energy transfer (FRET)- and chemiluminescence resonance energy transfer (CRET)-based sensing platforms (Zhu et al. 2013). More importantly, they are biocompatible and readily dispersed in aqueous solutions without surface modification or surfactants, making them suitable in biosensing applications.

Since the discovery of the double helix structure, nucleic acids have been employed in biosensors as recognition elements based on Watson-Crick base-pairing rules. In particular, the emergence of functional nucleic acids in the early 1980s further extends recognition capability (Guerrier-Takada et al. 1983; Kruger et al. 1982). Functional nucleic acids are specific oligonucleotides capable of folding into distinct three-dimensional structures and performing functions beyond carrying genetic information. Among them, aptamers are single-stranded oligonucleotides with specific recognition abilities through receptor-ligand interactions. Aptamers are selected by a technique known as “systematic evolution of ligands by exponential enrichment” (SELEX), and they exhibit high affinity towards a wide range of targets, such as small organic molecules, metal ions, proteins and cells (Ellington and Szostak 1990; Fang and Tan 2010; Tuerk and Gold 1990). Therefore, the introduction of aptamers can significantly expand the application scope of nucleic acid-based biosensors (Chen et al. 2011; Chen et al. 2015a; Shukoor et al. 2012; Tan et al. 2013; Yasun et al. 2012; Zheng et al. 2015). Metallo-base pairs also provide a feasible recognition strategy for biosensing. Through specific metal ion coordination between thymine (T) and Hg^{2+} or cytosine (C) and Ag^{+}, T-Hg^{2+}-T and C-Ag^{+}-C base pairs are formed with high stability (Miyake et al. 2006; Tanaka et al. 2002; Wagenknecht 2003). This strategy was employed in biosensors for selective detection of metal ions (Dave et al. 2010; Tortolini et al. 2015). In sum, owing to their powerful recognition properties, nucleic acid-based biosensors, especially aptasensors, have found a broad range of applications in the fields of bioanalysis and biomedicine e (Kong et al. 2011; Li et al. 2010; Liu et al. 2012; Lubin and Plaxco 2010; Tan et al. 2012; Tang et al. 2015; Wang et al. 2009; Zhao et al. 2015c).

The new wave to incorporate nanomaterials into biosensors has spawned many studies reporting on the integration of nucleic acids into transition metal nanosheet-based biosensors to improve sensing performance (Chen et al. 2015b; Wang et al. 2010; Yang et al. 2010; Zhu et al. 2015). Specifically, π-π stacking interaction between transition metal nanosheets and nucleic acids promotes facile assembly into biosensing systems. In addition, the high loading efficiency of nucleic acids can enhance biosensor sensitivity and recognition performance. Meanwhile, transition metal nanosheets can serve as carriers of nucleic acids, and by preventing nuclease degradation in complex environment, their many practical applications can be realized, in particular those involving clinical diagnostics. The first nucleic acid-functionalized transition metal nanosheet-based biosensor was reported by Zhu et al. (2013) for the detection of nucleic acids and small molecules. From then on, various biosensing systems have been continuously developed, with the scope of target analytes ranging from small molecules to large biomolecules (e.g., proteins). Besides detection in buffer solutions, driven by the needs of biomedicine and clinical diagnostics, increasing attention has been paid to the detection in more complex systems (e.g., living cells). Several research groups have successfully employed this system in intracellular imaging and detection (Jia et al. 2015; Zhao et al. 2014). Therefore, the combination of 2D transition metal nanomaterials and nucleic acids has resulted in many novel strategies for biosensing applications.

In this review, we provide an overview of nucleic acid-functionalized transition metal nanosheets in biosensing applications. The structure and properties of 2D transition metal nanomaterials are first discussed, emphasizing the interaction between transition metal nanosheets and nucleic acids. Next, we present recent progress in coupling nucleic acids and transition metal nanosheets to detect various targets in the context of different signal transducing mechanisms, including optical and electrochemical approaches. Finally, future perspectives and challenges are discussed.

2. Structure and properties of transition metal nanosheets

2D transition metal nanosheets are graphene analogues with atomic thickness and planar structure. Compared with graphene composed of only carbon, 2D transition metal nanomaterials constitute a large family and provide greater flexibility and diversity of composition, structure and functionality. TMCs are MX2-type compounds where M is a transition element of groups IV, V, and VI, and X is a chalcogen, such as S, Se, and Te (Doran 1980; Yoffe 1990). For example, layered MoS_2 consists of a sandwich structure of Mo atoms between two layers of S atoms, exhibiting strong in-plane covalent bonding and weak out-of-plane interaction, therefore enabling exfoliation from bulk 3D materials into 2D nanosheets (Ataca and Ciraci 2011; Brent et al. 2015; Huang et al. 2013b; Leonard and Talin 2011; Schwierz 2011). Single- or few-layer nanosheets present many attractive properties over their bulk counterparts and, as such, cater to wide applications in nanoelectronics (Lee et al. 2015; Radisavljevic et al. 2011a; Wu et al. 2014; Yin et al. 2012), catalysis (Chianelli et al. 2006; Gao et al. 2015; Huang et al. 2013a), energy harvesting (Jaramillo et al. 2007; Sun et al. 2014a) and biomedicine (Chen et al. 2015b; Cheng et al. 2014). On the other hand, TMOs are composed of oxygen atoms bound to transition metals. Generally, these oxide nanosheets exhibit high stability and tunable properties owing to diversity of chemical

composition and crystal structure (Geng et al. 2010; Ma et al. 2006; Osada and Sasaki 2009, 2012). For example, manganese, molybdenum and tungsten oxides possess facile redox activity (Ma and Sasaki 2010; Sasaki 2007), while titanium and zinc oxides show photocatalytic activity (McLaren et al. 2009; Wang and Sasaki 2014). Therefore, TMO nanosheets are widely applied in the fields of photocatalysis (Cai et al. 2015; Deng et al. 2015; Ebina et al. 2002; Shibata et al. 2007), optoelectronics (Osada and Sasaki 2009, 2012, 2015) and magneto-optics (Osada et al. 2006; Osada et al. 2008).

In addition to such exceptional properties, which make them attractive in the fields of electronics, catalysis, and energy harvesting, transition metal nanosheets are also gaining growing interest in the development of biosensors. As graphene analogues, TMCs and TMOs share many physiochemical properties in common with graphene, such as fluorescence quenching ability and physisorption towards single-stranded DNA (ssDNA) through **π**-**π** stacking interaction (Chen et al. 2012; Moses et al. 2009; Rurack 2001; Tang et al. 2010). MoS_2 is a typical family member of transition metal chalcogenides, and, taking it as an example, several studies have demonstrated the physisorption of aromatic (e.g., pyridine or purine) and conjugated compounds on the basal plane of MoS_2 (Heckl et al. 1991; Moses et al. 2009). Therefore, MoS_2 nanosheets could adsorb ssDNA via van der Waals interaction between nucleobases and basal plane of MoS_2. In contrast, double-stranded DNA (dsDNA) exhibits remarkably lower adsorption than ssDNA as a result of nucleobase shielding by helical phosphate backbones. Apart from DNA hybridization, it is worth pointing out that specific aptamer-target recognition can also weaken the adsorption of aptamer through 3D structural switching. Based on preferential adsorption towards random coil ssDNA, Zhang and coworkers first established a MoS_2 nanosheet-based sensing platform for the detection of DNA and small molecules (Zhu et al. 2013). Since then, other transition metal nanosheets, such as WS_2, TaS_2, CoS and MnO_2, have been found to exhibit similar physisorption and quenching abilities, and they have been successfully applied in biosensing systems.

In addition to the physical adsorption approach, nucleic acids can be immobilized on transition metal nanosheets through the decoration of metal nanoparticles. Gold nanoparticles (AuNP) are the most popular metal nanoparticles owing to their superior electrical and catalytic properties, as well as remarkable biocompatibility. The implementation of AuNPs can improve payload capacity for nucleic acids via Au–S bond self-assembly. On the other hand, AuNPs can also amplify electrochemical signals by accelerating electron transfer, and since poor conductivity is one of the obstacles hindering electrochemical applications of transition metal nanomaterials, this feature is of singular importance (Meng et al. 2013). For example, Huang et al. (2014a) coupled AuNPs with WS_2-graphene nanosheet/ glassy carbon electrode (GCE), and based on the synergistic effect of WS_2-graphene nanosheets and AuNPs, the as-prepared biosensor demonstrated increased effective active area of electrode and enhanced electrochemical signal.

Furthermore, transition metal nanosheets could serve as a carrier for nucleic acid payloads, as well as protect against nuclease degradation in complex conditions, thus facilitating their biosensing performance in practical applications. Recently, our group reported a MnO_2 nanosheet-aptamer nanoprobe for dual-activatable fluorescence/MRI bimodal tumor imaging

(Zhao et al. 2014). In this study, dye-labeled aptamers capable of selectively recognizing specific tumor cells are adsorbed on MnO_2 nanosheets, while redoxable MnO_2 nanosheets serve as aptamer nanocarrier, fluorescence quencher and MRI contrast agent. In the presence of target cells, the interaction between aptamers and their targets induces desorption of aptamers and uptake of nanosheets into target cells. During this process, fluorescence recovery is observed by the dissociation of dye molecules from nanosheets. Meanwhile, endocytosed MnO_2 nanosheets are subsequently reduced by intracellular glutathione, generating a large amount of Mn^{2+} for MRI signal. In the absence of target cells, neither fluorescence nor MRI signal is activated. Later, our group also demonstrated that DNAzyme adsorbed on MnO_2 nanosheets can provide protection against enzymatic digestion and provide efficient delivery into cytoplasm (Fan et al. 2015).

3. Nucleic acid-functionalized transition metal nanosheets for optical detection

Transition metal nanosheets have a natural gift as fluorescence nanoquenchers, which is achieved through energy-transfer or electron-transfer from excited fluorophores to nanosheets. In addition, their large surface area offers more quenching sites, thus providing enhanced quenching performance and detection sensitivity. Therefore, transition metal nanosheets can serve as energy acceptors in biosensor construction based on FRET or CRET. Meanwhile, TMCs, such as MoS_2, WS_2 and WSe_2, were found to exhibit strong photoluminescence from their direct-gap electronic structures. Taking advantage of such quenching abilities and intrinsic photoluminescence, a variety of optical sensing strategies have been implemented to detect nucleic acids, proteins and small molecules.

3.1 Detection of nucleic acids

Sensitive, selective, rapid, and cost-effective analysis of nucleic acids plays a critical role in medical diagnostics, genetic and environmental monitoring, drug discovery and food safety (McCarthy and Hilfiker 2000; Velusamy et al. 2010). Based on specific adsorption properties towards nucleic acids, transition metal nanosheets are widely employed for nucleic acid detection.

In 2013, Zhang and coworkers first reported that MoS_2 nanosheets possess fluorescence quenching capability and different affinity towards ssDNA and dsDNA (Zhu et al. 2013). Based on this finding, MoS_2 nanosheets were employed in a DNA sensing platform. As shown in Figure 1A, a dye-labeled ssDNA was adsorbed on MoS_2 nanosheets with quenched fluorescence. However, upon addition of the complementary target DNA, hybridization weakened the van der Waals interaction between nucleobases and nanosheet, leading to desorption of DNA strand and restoration of fluorescence. This MoS_2 nanosheet-based biosensor exhibited excellent performance for rapid and homogeneous analysis of DNA, with a detection limit of 500 pM. The author further demonstrated the versatility of this platform by using an adenosine aptamer as probe DNA, and a detection limit of 5 μM was achieved.

Inspired by exceptional performance of the MoS_2 nanosheet-based biosensor and considering physical and chemical properties shared in common by transition metal nanomaterials, researchers found that other transition metal nanosheets, such as WS_2 (Yuan et al. 2014a), MnO_2 (He et al. 2014; Wang et al. 2015a) and Ta_2NiS_5(Tan et al. 2015) nanosheets, also exhibit high quenching efficiency and physisorption properties towards dye-labeled ssDNA. As a consequence, these 2D nanomaterials have also been employed for biomolecule detection. Typically, the Zhang group further adapted the sensing platform for multiplexed DNA detection by simultaneously adsorbing two different ssDNA probes targeting Influenza A virus subtype H1N1 gene and subtype H5N1 gene onto TaS_2 nanosheets. The probes only responded to specific target sequence and emitted corresponding fluorescence (Zhang et al. 2015).

Several adaptions have since been made to this sensing platform to improve biosensor performance. For instance, Wang et al. (2015b) first used a peptide nucleic acid (PNA) probe, instead of a DNA probe, in a WS_2 nanosheet-based platform, owing to higher binding affinity and sequence specificity of PNA/DNA hybridization. This platform shows lower background signal and greater discrimination of single-base mismatch. Huang et al. (2015a) coupled the MoS_2 nanosheet-based biosensor with hybridization chain reactions (HCR) for improved sensitivity, achieving a detection limit of 15 pM. In addition, this assay can be further integrated into a microfluidic device for heterogeneous and high-throughput detection of DNA. The use of microfluidics significantly reduced sample volume, thereby achieving detection of 0.5 fmol target DNA in a visible manner within minutes (Huang et al. 2015d).

Besides different affinities towards ssDNA and dsDNA, it was also revealed that short oligonucleotide fragments (<10 bases) and ssDNA (<10 bases) exhibit different interactions with WS_2 nanosheets. Based on this finding, Jiang and coworkers developed a WS_2-based biosensing platform coupled with duplex-specific nuclease signal amplification (DSNSA) for microRNA (miRNA) detection (Xi et al. 2014). As shown in Figure 1B, dye-labeled ssDNA probe was designed to be complementary to target miRNA, and the resulting heteroduplex was cleaved by duplex-specific nuclease. Resulting from changes in length, as well as the secondary structure, the cleaved DNA probe exhibited weak affinity towards WS_2 nanosheets and was barely adsorbed onto the nanosheets, thereby recovering fluorescence. However, in the absence of target miRNA, the full-length DNA probe strongly adsorbed onto nanosheets, and the fluorescence was almost entirely quenched. Taking advantage of such signal amplification strategy, this method showed enhanced sensitivity with a detection limit of 300 fM.

Apart from FRET-based biosensors, transition metal nanosheets have also been incorporated into CRET systems for nucleic acid detection. Zhao et al. (2015a) reported a novel WS_2 nanosheet-based CRET platform to detect miRNA. Using an ssDNA probe containing a G-quadruplex-hemin DNAzyme structure adsorbed onto the WS_2 nanosheets, the chemiluminescence produced by the G-quadruplex-hemin-H_2O_2-luminol system was quenched by the WS_2 nanosheet as a result of its broad light absorption. Upon addition of target miRNA, which hybridized with the 3’-end of the DNA probe to form a stable RNA/DNA heteroduplex, DNAzyme was dissociated from the nanosheets, and a strong

chemiluminescence signal was observed. The restoration of chemiluminescence and the concentration of target miRNA showed a linear relationship, ranging from 0.5 to 10 nM, with a detection limit of 180 pM (3σ) (Fig. 1C).

As mentioned above, in addition to acting as a fluorescence nanoquencher, several transition metal nanosheets possessed intrinsic photoluminescence (Rao et al. 2013). Taking advantage of this property, Loan et al. (2014) developed a graphene/MoS_2 heterostructure to detect DNA hybridization. In this work, graphene serves as a biocompatible interface layer to host DNA molecules, as well as provide a protective layer to prevent undesirable reaction between MoS_2 and ambient environment. The photoluminescence intensity of MoS_2 increases as the amount of positive charge increases in the presence of target DNA. Moreover, the introduction of graphene reduces the electron concentrations of MoS_2 nanosheets, thereby increasing the sensitivity of this system. The photoluminescence intensity of MoS_2 positively correlates with the concentration of target DNA, with a detection limit of 1 aM (10^{-18} M).

3.2 Detection of proteins

Proteins play vital roles in regulating various physiological functions. Sensitive protein detection is critical in medical diagnostics and therapy (Tan et al. 2014; Tyrakowski and Snee 2014; Zhou et al. 2012). Aptamers possess several advantages over antibodies in protein recognition and detection, such as *in vitro* synthesis, chemical stability, low immunogenicity and flexible fabrication (Bunka and Stockley 2006; Famulok et al. 2007; Osborne et al. 1997). Moreover, according to the universal principle described above, the transition metal nanosheet-based biosensing platform is suitable for various types of protein detection by using dye-labeled aptamer probes. The interaction between aptamers and their target proteins induces a rigid conformation, which impairs the affinity between aptamer probes and nanosheets, leading to the desorption of probe DNA and restoration of fluorescence signal (Ge et al. 2014a; He et al. 2014; Kong et al. 2015; Wang et al. 2015a; Yuan et al. 2014a; Zhu et al. 2013). For example, Ge et al. (2014a) developed a novel biomolecule sensor by adsorbing thrombin aptamer onto MoS_2 nanosheets. Kong et al. (2015) employed prostate specific antigen (PSA) aptamer as the recognition unit for sensitive detection of PSA, and the constructed biosensor was successfully applied in human serum samples. Yin et al. (2015) reported a VS_2 nanosheet-based biosensor for detection of cytochrome c.

Apart from using aptamers, another strategy employed for protein detection involves the conversion of protein assay into highly sensitive detection of DNA (Ge et al. 2014b; Liu et al. 2014a; Wang et al. 2015a; Xiang et al. 2015; Zhao et al. 2015b). To accomplish this, Xiang et al. developed a novel fluorescence biosensor for streptavidin (SA) detection by combining the terminal protection of small-molecule-linked DNA (TPSMLD) and exonuclease III (Exo III)-aided DNA recycling amplification (Xiang et al. 2015). As shown in Figure 2, a biotin-linked probe 1 and a FAM-labeled probe 2 were used in this study, and probe 2 was tethered to the 3’-end of the antisense strand of probe 1. In the absence of SA, ssDNA probe 2 was firmly adsorbed onto MoS_2 nanosheets, emitting a low fluorescence signal. In the presence of SA, the specific binding of SA to biotinylated molecule avoided

the degradation of probe 1 by Exo I, and the addition of probe 2 resulted in the formation of DNA duplex. Meanwhile, since probe 2 was hydrolyzed by Exo III, leaving ssDNA probe 1 to the next signal generation cycle, releasing more probe 2 from the nanosheet surface and recovering the fluorescence signal. The detection limit reached 0.67 ng/mL.

T4 polynucleotide kinase (PNK) phosphorylates DNA at the 5'-hydroxyl termini by catalyzing the transfer of λ-phosphate residue of ATP to nucleic acids, playing an important role in many cellular events (Becker and Hurwitz 1967; Cameron and Uhlenbeck 1977). Several attempts have been made to detect the activity of T4 PNK (Ge et al. 2014b; Liu et al. 2014a). In particular, Ge et al. (2014b) succeeded in developing a WS_2 nanosheet-based biosensor to analyze the activity of T4 PNK. As shown in Figure 3, a FAM-labeled dsDNA was phosphorylated in the presence of T4 PNK, which was promptly digested by λ exonuclease to yield a FAM-labeled ssDNA. Addition of WS_2 nanosheet could substantially quench the fluorescence of FAM because of the interaction between ssDNA and nanosheet. However, in the absence of T4 PNK, the 5'-hydroxyl group prohibited cleavage, and since the remaining dsDNA had weak affinity towards WS_2 nanosheets, a strong fluorescence signal was observed. This assay for T4 PNK activity offers a low detection limit of 0.01 U/mL with a linear range from 0.01 to 10 U/mL.

The fluorescence polarization (FP) assay is a convenient fluorescent technique widely applied in the detection of various biomolecules (Jameson and Ross 2010). Zhao et al. (2015b) developed a WS_2 nanosheet-based sensing platform coupled with Exo III co-assisted signal amplification for highly sensitive fluorescence polarization analysis of DNA glycosylase activity. The FP value correlates with the mass of FAM fluorophores labeled on probe DNA, which is affected by the adsorption and desorption of DNA probe onto WS_2 nanosheets. This strategy exhibited excellent sensitivity with a detection limit of 0.00030 U/mL.

3.3 Detection of small molecules and metal ions

The successful applications of transition metal nanosheets in detecting nucleic acids and proteins have sparked new interest in developing novel transition metal nanosheet-based biosensors for different targets. Since aptamers have a board range of targets, including various important organic small molecules, such as intracellular biomolecules and drug molecules, aptamer-functionalized transition metal nanosheet-based biosensors can also be used to detect small molecules. Using this strategy, Jia et al. (2015) synthesized a smart MoS_2-based nanoprobe by adsorbing ATP aptamer onto MoS_2 nanosheets for *in situ* monitoring of intracellular ATP.

In addition to fluorescence dye, emissive nanoparticles are also quenched by some transition metal nanosheets. Liu and coworkers first revealed that the fluorescence emission of upconversion nanoparticles was quenched by MnO_2 nanosheets when MnO_2 was coated on the surface of the nanoparticles (Deng et al. 2011). Based on this finding, Yuan et al. (2014b) employed MnO_2 nanosheets as a label-free biosensor for homogeneous sensing applications. As shown in Figure 4A, ochratoxin A (OTA) aptamers tethered to upconversion nanoparticles are assembled on the MnO_2 nanosheet, resulting in the fluorescence quenching of upconversion luminescence through energy transfer from the fluorophore to MnO_2. Upon

addition of the target molecule OTA, the aptamer undergoes conformational changes which weaken the interaction between nucleobases and nanosheets, making it possible to observe desorption of upconversion nanoparticles and the recovery of fluorescence. These sensors can be applied in both aqueous solutions and complex samples with a detection limit of 0.02 ng/mL.

Quantitatively monitoring the level of drug molecules is important in disease therapy and related mechanistic research. Bleomycin (BLM) is a widely used antitumor drug. In the presence of Fe(II), it has been reported that bleomycin forms a BLM Fe(II) complex, which could further interact with oxygen to generate an active BLM Fe(III)OOH complex capable of catalyzing the incision of DNA (Claussen and Long 1999). Based on this scission ability, Qin et al. (2015) developed a simple and sensitive WS_2 nanosheet-based sensing platform for bleomycin detection. In this work, a FAM-labeled long ssDNA was adsorbed on WS_2 nanosheet with the fluorescence of FAM quenched. However, the addition of BLM Fe(II) complex induced an irreversible scission of long ssDNA, and the resulting short ssDNA tagged with FAM was barely adsorbed on nanosheet, thus retaining a strong fluorescence emission. In this construct, fluorescence recovery is related to the concentration of bleomycin and displays a wide linear range with a detection limit of 0.3 nM (see Fig. 4B).

In addition to organic small molecules, various metal ion biosensors have been explored based on the specific interaction between metal ions and nucleic acids, especially T-Hg^{2+}-T base pairs and C-Ag^{+}-C base pairs. Therefore, such metallo-base pairs can also be implemented for use in transition metal nanosheet-based biosensors to detect metal ions. Yang et al. (2014a) proposed a rapid and simple detection of Hg^{2+} ions by using MnO_2 nanosheets and FAM-labeled T-rich sequences. As shown in Figure 5, in the absence of Hg^{2+}, the probe DNA adopts a random coil able to easily interact with MnO_2 nanosheets and quench fluorescence. In contrast, in the presence of Hg^{2+}, the coordination between Hg^{2+} and thymine bases yields a rigid hairpin structure, with little chance of adsorption onto MnO_2 nanosheets, thereby retaining fluorescence. Also, by choosing a cytosine-rich sequence as the probe, highly sensitive and selective detection of Ag^{+} could be achieved using a similar strategy (Mao et al. 2015).

4. Nucleic acid-functionalized transition metal nanosheets for electrochemical detection

Electrochemical biosensors are known to possess many advantages, including simplicity, low-cost, high selectivity and sensitivity (Wang et al. 2013). Based on their exceptional physical and electrochemical properties, two-dimensional transition metal nanomaterials are attracting increasing attention in electrochemical sensing. For example, bulk WS_2 is generally an n-type semiconductor with an indirect bandgap (~1.4 eV), while monolayer WS_2 has a direct bandgap of ~1.9 eV (Wang et al. 2012). Meanwhile, MoS_2 has sparked tremendous interest in recent years. Several groups have shown that a single-layer of MoS_2 has a direct bandgap up to 1.90 eV (Braga et al. 2012). Recently, 2D-layered transition metal nanomaterials have been successfully applied in the development of electrochemical sensors (Su et al. 2015).

4.1 Detection of nucleic acids

Compared with optical detection of nucleic acids that commonly use dye-labeled DNA probes, electrochemical assays employing transition metal nanosheets provide a label-free platform with faster and simpler detection, while, at the same time, reducing the uncertainty induced by labels. Recently, Wang et al. (2015c) developed a label-free and ultrasensitive electrochemical DNA sensor based on thin-layer molybdenum disulfide (MoS_2) nanosheets. In this work, thin-layer MoS_2 nanosheets with enhanced electrochemical activity were prepared by ultrasound exfoliation. Based on different affinities towards ssDNA versus dsDNA of the MoS_2 nanosheets, methyl blue (MB) was chosen as the indicator to monitor the changes of electrode surface induced by DNA immobilization and hybridization. The target gene sequence related to *Vibrio parahaemolyticus* could be detected from 1.0×10^{-16} M to 1.0×10^{-10} M with a detection limit of 1.9×10^{-17} M.

On the other hand, MoS_2 nanoflakes can be used as inherently electroactive labels with the inherent oxidation peak exploited as the analytical signal. MoS_2 nanoflakes could effectively adsorb the immobilized ssDNA probe via van der Waals force interaction. When ssDNA probe underwent hybridization with its complementary DNA to form dsDNA, the degree of interaction between the resulting dsDNA duplex and MoS_2 nanoflakes was reduced. Therefore, more MoS_2 nanoflakes were conjugated with the ssDNA probe-modified disposable electrical printed (DEP) chip surface relative to the dsDNA duplex-modified DEP chip surface and, thus, a greater voltammetric signal, stemming from the oxidation of MoS_2 nanoflakes, was achieved for ssDNA. The concentration of the DNA probe immobilized onto the DEP chip surface was determined to be 10 μM, while the concentration of MoS_2 nanoflakes was 0.018 mg/mL. Under the optimized conditions, the range of detection was determined to be from 0.03 nM to 300 nM with good linearity (see Fig. 6) (Loo et al. 2014).

Thus far, the electrochemical application of transition metal nanosheets has suffered from poor conductivity. To overcome this obstacle, other conducting materials, such as graphene (Huang et al. 2014b), multi-walled carbon nanotube (MWCNT) (Huang et al. 2014c) and AuNPs (Huang et al. 2014b; Huang et al. 2014c), have been combined with transition metal nanosheets. For example, Huang and coworkers reported an electrochemical DNA biosensor based on MoS_2/MWCNT nanocomposites coupled with AuNP signal amplification and an enzyme-assisted signal amplification strategy. In this work, a MoS_2/MWCNT and AuNP-modified electrode coupled with glucose oxidase (GOD) was assembled with a thiol-tagged DNA probe. The MoS_2/MWCNT heteronanostructure exhibited good conductivity for accelerating electron transfer, while GOD served as a redox marker generating DET signal. Meanwhile, the modification of GOD and AuNPs provided enzyme-assisted signal amplification for biosensing. The multiple signal amplification strategy exhibited a detection limit to 0.79 fM with a linear range from10 fM to 10^7 fM. This DNA biosensor also showed good discrimination of single-base mismatch, three-base mismatch and noncomplementary DNA.

4.2 Detection of proteins

Electrochemical assays provide a fast, simple and inexpensive method of detecting proteins (Erdem and Congur 2014; Yang et al. 2014b). However, ultrasensitive detection at ultra-trace

level remains an obstacle. In this situation, aptamers are promising candidates for target recognition. Huang et al. (2014a) reported a label-free electrochemical assay for sensitive determination of immunoglobulin E (IgE) by assembling aptamers on a glassy carbon electrode (GCE) modified with WS_2-graphene nanosheets and AuNPs. The WS_2-graphene nanosheet acted as a good electrical conductor for accelerating electron transfer, while the modification of AuNPs provided a large electroactive surface area for electrochemical detection. The detection of IgE was performed by measuring the electrochemical signal response of $[Fe(CN)6]^{3-/4-}$ using differential pulse voltammetry (DPV). The peak current and the logarithm of IgE concentration displayed a linear relationship range from 1.0×10^{-12} to 1.0×10^{-8} M with a detection limit of 1.2×10^{-13} M (3σ/S) (see Fig. 7).

In order to improve detection sensitivity, Jing et al. (2015) developed a signal-amplified sandwich-type electrochemical aptasensor fabricated for selective quantification of thrombin based on palladium nanoparticles (PdNPs)/poly(diallyldimethylammonium chloride (PDDA)-graphene-MoS_2 flower-like nanocomposites and enzymatic signal amplification. As shown in Figure 8, the primary aptamer of thrombin (TBA) was assembled on an Au electrode surface through Au-N affinity, while PdNPs/PDDA-graphene-MoS_2 served as a nanocarrier to load large amounts of the electron transfer mediator toluidine blue (Tb), which was further functionalized by hemin/G-quadruplex and GOD as the secondary aptamer. The target protein thrombin was sandwiched between the primary aptamer and the prepared secondary aptamer to fabricate the sandwich-type electrochemical aptasensor. GOD, PdNPs and hemin/G-quadruplex could amplify the electrochemical signal through synergetic catalysis. The proposed aptasensor for thrombin detection showed high sensitivity with a linear range of 0.1 pM to 40 nM and a low detection limit of 0.062 pM.

Several attempts have also been made to couple different nanoparticles for signal-amplified detection of proteins, taking advantages of their large electroactive surface area, high electron transfer characteristics and high electrochemical stability. For instance, Fang et al. (2015) reported an electrochemical aptasensor for PDGF-BB detection, combining MoS_2/carbon aerogel composites and AuNPs for signal amplification. Liu et al. (2014b) developed a thrombin aptasensor using MoS_2 nanosheet-graphene composites and AuNPs for signal amplification.

4.3 Detection of small molecules

The detection of small molecules is related to many biological process and diseases. Nucleic acid-functionalized transition metal nanosheet-based biosensors are also employed in the determination of various small molecules. 17β-estradiol, for example, has been listed as a typical environmental endogenous estrogen which can disrupt the endocrine system, leading to adverse effects on normal physiological processes. Huang and coworkers reported an electrochemical biosensor for 17β-estradiol by assembling an aptamer on AuNPs/CoS-modified GCE (Huang et al. 2015c). As shown in Figure 9, the CoS/AuNPs film, which formed on the biosensor surface, served as a good conductor for accelerating electron transfer and enhancing the detection signal. MB was applied as an indicator, and a guanine-rich complementary DNA was designed to bind with unbound aptamer for signal amplification. Hybridization between guanine-rich DNA and aptamer was inhibited in the

presence of 17β-estradiol by aptamer-target interaction. The use of guanine-rich DNA significantly amplified the redox signal of MB bound to the detection probe. Under the optimized conditions, this 17β-estradiol biosensor demonstrated a detection range from 1.0×10^{-9} to 1.0×10^{-12} M with a detection limit of 7.0×10^{-13} M. Furthermore, the biosensor exhibited good selectivity towards 17β-estradiol, even when some potential interferents were presented at 100-fold concentrations. The same group also developed other two aptasensors for 17β-estradiol detection, using layered tungsten disulfide nanosheets/Au nanoparticles (Huang et al. 2015b) and copper sulfide nanosheets/Au nanoparticles (Huang et al. 2014d) for signal amplification, respectively.

Riboflavin (6, 7-dimethyl-9-(d-1-ribityl)-*izo*-alloxazine), commonly called vitamin B2, is one of the most widely used vitamins. Wang et al. (2015d) developed an electrochemical sensor based on a 32-mer homoadenine ssDNA/molybdenum disulfide-graphene nanocomposite-modified gold electrode (MoS_2-graphene/A32/Au electrode). The obtained electrode was used as a probe for DPV sensing of riboflavin. The linear detectable ranges were from 0.025μM to 2.25μM, and the limit of detection (LOD, S/N=3) was 20 nM. Moreover, the MoS_2-graphene/A32/Au electrode could be successfully used for riboflavin detection in urine samples.

5. Conclusion and perspectives

In this review, we have presented an overview of recent advances in nucleic acid-functionalized transition metal nanosheets for biosensing applications. Taking advantage of the unique physicochemical properties of 2D transition metal nanomaterials and the powerful recognition abilities of nucleic acids, the combination of these two components provides new insights into biosensing. Various targets, including nucleic acids, proteins, orgainc small molecules, metal ions and even cells can be detected using nucleic acid-functionalized transition metal nanosheet-based biosensors with high selectivity, high sensitivity, fast detection time, easy operation, and low cost.

In spite of remarkable progress, the exploration of these biosensors in practical applications remains challenging. Currently, most of the reported results are performed in optimal laboratory conditions as proof-of-concept. However, in the case of complex environment (e.g., blood and urine), a mixture of biomolecules and ions may induce false signals and reduced sensitivity (Chiu et al. 2010). For instance, ssDNA adsorbed onto nanosheets could be displaced by nonspecific interaction between nanosheets and biomolecules in complex environment, leading to false signals. Additionally, several studies have reported that nanoparticles tend to aggregate in complex condition (French et al. 2009; Keller et al. 2010). Therefore, more emphasis should be placed on evaluating feasibility and performance in complex environments. To move this field forward, a substantial amount of work remains to be done. First, from a materials point of view, controllable, reproducible and scalable synthesis of transition metal nanosheets with desired physicochemical properties will significantly improve their optical and electrochemical sensing performance. Hence, precise control of nanomaterial synthesis, together with an in-depth insight of synthesis mechanism, deserves more intensive research. Furthermore, current studies mainly focus on limited materials, such as MoS_2, WS_2 and MnO_2. Since transition metal nanomaterials constitute a

large family, making full use of other transition metal nanomaterials, or constructing hybrid nanostructures based on different family members, will bring intriguing properties and promising applications.

Undoubtedly, the integration of various functional nucleic acids (e.g., aptamers and DNAzyme) into transition metal nanosheet-based biosensors has extended the avenues for biosensor development (Liu et al. 2009). However, in complex environments, genetic materials face the additional limitation of instability. However, the use of artificial nucleic acids, such as PNA and locked nucleic acid (LNA), or chemical modifications of nucleic acids, such as 2′-*O*-methyl modification and phosphorothioate modification, may overcome the instability. Meanwhile, nucleic acids offer intrinsic design flexibility with easy modification of nucleobase and DNA strands. The introduction of nucleic acids modified with functional moieteis or containing unnatural nucleotides will further introduce various functional groups. Thus, multiplexed and multimodal biosensing can be realized by combining different capabilities and merits. Additionally, as mentioned above, the adsorption/desorption of nucleic acids on nanosheets is critical for reducing background signals and enhancing detection sensitivity. Therefore, a better understanding of the interaction between nucleic acids and nanosheets will lead to better biosensing performance. By improving the stability and effectiveness of biosensors, it is anticipated that detection in complex conditions can be achieved.

The applications of biosensors for *in vivo* detection and imaging hold great promise in biomedical and clinical research. To realize *in vivo* biosensing, more attention should be given to the instability, targeting specificity and biosafety effects of biosensors. It is well known that biological barriers are presented by the *in vivo* environment, such as nonspecific accumulation of nanosheets on nontarget sites by the lack of targeting specificities. Biosafety is also an important issue to consider before undertaking applications *in vivo*. To this end, exploring nanomaterials with low toxicity and appropriate surface modifications to nanosheets is necessary. Additionally, although current acute toxicity evaluations have demonstrated low toxicities of several transition metal nanosheets, more emphasis should be placed on evaluating long-term toxicity, including biodistribution and metabolism assessments, while the toxicity tests should be extended from cellular level to tissue level. With rapid development of nanotechnology and life sciences, it is anticipated that advancements in nucleic acid-functionalized transition metal nanosheet-based biosensors will have increasing impact on biological studies, diagnosis and environmental monitoring in the future.

Acknowledgments

This work was supported by the National Key Scientific Program of China (2011CB911000), the National Key Basic Research Program of China (2013CB932702), NSFC (Grants 21327009, 21221003), National Instrumentation Program (2011YQ030124).

References

Ataca C, Ciraci S. J. Phys. Chem. C. 2011; 115:13303–13311.
Becker A, Hurwitz J. J. Biol. Chem. 1967; 242:936–950. [PubMed: 4289819]
Braga D, Lezama IG, Berger H, Morpurgo AF. Nano Lett. 2012; 12:5218–5223. [PubMed: 22989251]

Brent JR, Lewis DJ, Lorenz T, Lewis EA, Savjani N, Haigh SJ, Seifert G, Derby B, O'Brien P. J. Am. Chem. Soc. 2015; 137:12689–12696. [PubMed: 26352047]

Bunka DHJ, Stockley PG. Nat. Rev. Microbiol. 2006; 4:588–596. [PubMed: 16845429]

Cai XK, Sakai N, Ozawa TC, Funatsu A, Ma RZ, Ebina Y, Sasaki T. ACS Appl. Mater. Interfaces. 2015; 7:11436–11443. [PubMed: 25945510]

Cameron V, Uhlenbeck OC. Biochemistry. 1977; 16:5120–5126. [PubMed: 199248]

Chen D, Feng H, Li J. Chem. Rev. 2012; 112:6027–6053. [PubMed: 22889102]

Chen T, Shukoor MI, Chen Y, Yuan Q, Zhu Z, Zhao Z, Gulbakan B, Tan W. Nanoscale. 2011; 3:546–556. [PubMed: 21109879]

Chen TT, Tian X, Liu CL, Ge J, Chu X, Li YF. J. Am. Chem. Soc. 2015a; 137:982–989. [PubMed: 25548948]

Chen Y, Tan C, Zhang H, Wang L. Chem. Soc. Rev. 2015b; 44:2681–2701. [PubMed: 25519856]

Cheng L, Liu J, Gu X, Gong H, Shi X, Liu T, Wang C, Wang X, Liu G, Xing H, Bu W, Sun B, Liu Z. Adv. Mater. 2014; 26:1886–1893. [PubMed: 24375758]

Chhowalla M, Shin HS, Eda G, Li L-J, Loh KP, Zhang H. Nat. Chem. 2013; 5:263–275. [PubMed: 23511414]

Chianelli RR, Siadati MH, De la Rosa MP, Berhault G, Wilcoxon JP, Bearden R, Abrams BL. Catal. Rev. 2006; 48:1–41.

Chiu ML, Lawi W, Snyder ST, Wong PK, Liao JC, Gau V. Jala-J. Lab. Autom. 2010; 15:233–242.

Claussen CA, Long EC. Chem. Rev. 1999; 99:2797–2816. [PubMed: 11749501]

Dave N, Chan MY, Huang P-JJ, Smith BD, Liu J. J. Am. Chem. Soc. 2010; 132:12668–12673. [PubMed: 20726570]

Deng Q, Tang HB, Liu G, Song XP, Xu GP, Li Q, Ng DHL, Wang GZ. Applied Surface Science. 2015; 331:50–57.

Deng R, Xie X, Vendrell M, Chang Y-T, Liu X. J. Am. Chem. Soc. 2011; 133:20168–20171. [PubMed: 22107163]

Doran NJ. Physica B & C. 1980; 99:227–237.

Ebina Y, Sasaki T, Harada M, Watanabe M. Chem. Mater. 2002; 14:4390–4395.

Ellington AD, Szostak JW. Nature. 1990; 346:818–822. [PubMed: 1697402]

Erdem A, Congur G. Sens. Actuators B. 2014; 196:168–174.

Famulok M, Hartig JS, Mayer G. Chem. Rev. 2007; 107:3715–3743. [PubMed: 17715981]

Fan H, Zhao Z, Yan G, Zhang X, Yang C, Meng H, Chen Z, Liu H, Tan W. Angew. Chem. Int. Ed. 2015; 54:4801–4805.

Fang L-X, Huang K-J, Liu Y. Biosens. Bioelectron. 2015; 71:171–178. [PubMed: 25909336]

Fang X, Tan W. Acc. Chem. Res. 2010; 43:48–57. [PubMed: 19751057]

French RA, Jacobson AR, Kim B, Isley SL, Penn RL, Baveye PC. Environ. Sci. Technol. 2009; 43:1354–1359. [PubMed: 19350903]

Gao MR, Chan MKY, Sun YG. Nat. Commun. 2015; 6:7493. [PubMed: 26138031]

Ge J, Ou E-C, Yu R-Q, Chu X. J. Mater. Chem. B. 2014a; 2:625–628.

Ge J, Tang L-J, Xi Q, Li X-P, Yu R-Q, Jiang J-H, Chu X. Nanoscale. 2014b; 6:6866–6872. [PubMed: 24830570]

Geng F, Ma R, Sasaki T. Acc. Chem. Res. 2010; 43:1177–1185. [PubMed: 20560546]

Goswami N, Giri A, Pal SK. Langmuir. 2013; 29:11471–11478. [PubMed: 23931064]

Guerrier-Takada C, Gardiner K, Marsh T, Pace N, Altman S. Cell. 1983; 35:849–857. [PubMed: 6197186]

He D, He X, Wang K, Yang X, Yang X, Li X, Zou Z. Chem. Commun. 2014; 50:11049–11052.

Heckl WM, Smith DP, Binnig G, Klagges H, Hansch TW, Maddocks J. Proc. Natl. Acad. Sci. USA. 1991; 88:8003–8005. [PubMed: 1896446]

Huang J, Ye L, Gao X, Li H, Xu J, Li Z. J. Mater. Chem. B. 2015a; 3:2395–2401.

Huang K-J, Liu Y-J, Cao J-T, Wang H-B. Rsc Adv. 2014a; 4:36742–36748.

Huang K-J, Liu Y-J, Wang H-B, Gan T, Liu Y-M, Wang L-L. Sens. Actuators B. 2014b; 191:828–836.

Huang K-J, Liu Y-J, Wang H-B, Wang Y-Y, Liu Y-M. Biosens. Bioelectron. 2014c; 55:195–202. [PubMed: 24384259]

Huang K-J, Liu Y-J, Zhang J-Z. Microchim. Acta. 2015b; 182:409–417.

Huang K-J, Liu Y-J, Zhang J-Z, Cao J-T, Liu Y-M. Biosens. Bioelectron. 2015c; 67:184–191. [PubMed: 25155132]

Huang K-J, Liu Y-J, Zhang J-Z, Liu Y-M. Anal. Methods. 2014d; 6:8011–8017.

Huang X, Zeng Z, Bao S, Wang M, Qi X, Fan Z, Zhang H. Nat. Commun. 2013a; 4:1444.

Huang X, Zeng Z, Zhang H. Chem. Soc. Rev. 2013b; 42:1934–1946. [PubMed: 23344899]

Huang Y, Shi Y, Yang HY, Ai Y. Nanoscale. 2015d; 7:2245–2249. [PubMed: 25567642]

Jameson DM, Ross JA. Chem. Rev. 2010; 110:2685–2708. [PubMed: 20232898]

Jaramillo TF, Jorgensen KP, Bonde J, Nielsen JH, Horch S, Chorkendorff I. Science. 2007; 317:100–102. [PubMed: 17615351]

Jia L, Ding L, Tian J, Bao L, Hu Y, Ju H, Yu J-S. Nanoscale. 2015; 7:15953–15961. [PubMed: 26367253]

Jing P, Yi H, Xue S, Chai Y, Yuan R, Xu W. Anal. Chim. Acta. 2015; 853:234–241. [PubMed: 25467464]

Keller AA, Wang H, Zhou D, Lenihan HS, Cherr G, Cardinale BJ, Miller R, Ji Z. Environ. Sci. Technol. 2010; 44:1962–1967. [PubMed: 20151631]

Kong R-M, Ding L, Wang Z, You J, Qu F. Anal. Bioanal. Chem. 2015; 407:369–377. [PubMed: 25366976]

Kong R-M, Zhang X-B, Chen Z, Tan W. Small. 2011; 7:2428–2436. [PubMed: 21726041]

Kruger K, Grabowski PJ, Zaug AJ, Sands J, Gottschling DE, Cech TR. Cell. 1982; 31:147–157. [PubMed: 6297745]

Lee HS, Baik SS, Lee K, Min S-W, Jeon PJ, Kim JS, Choi K, Choi HJ, Kim JH, Im S. ACS Nano. 2015; 9:8312–8320. [PubMed: 26169189]

Lembke D, Bertolazzi S, Kis A. Acc. Chem. Res. 2015; 48:100–110. [PubMed: 25555202]

Leonard F, Talin AA. Nat. Nanotechnol. 2011; 6:773–783. [PubMed: 22120529]

Li D, Song S, Fan C. Acc. Chem. Res. 2010; 43:631–641. [PubMed: 20222738]

Li H, Yin Z, He Q, Li H, Huang X, Lu G, Fam DWH, Tok AIY, Zhang Q, Zhang H. Small. 2012; 8:63–67. [PubMed: 22012880]

Liu J, Cao Z, Lu Y. Chem. Rev. 2009; 109:1948–1998. [PubMed: 19301873]

Liu J, Liu H, Kang H, Donovan M, Zhu Z, Tan W. Anal. Bioanal. Chem. 2012; 402:187–194. [PubMed: 22052153]

Liu J, Lu Y. J. Am. Chem. Soc. 2007; 129:9838–9839. [PubMed: 17645334]

Liu X, Ge J, Wang X, Wu Z, Shen G, Yu R. Anal. Methods. 2014a; 6:7212–7217.

Liu Y-M, Zhou M, Liu Y-Y, Huang K-J, Cao J-T, Zhang J-J, Shi G-F, Chen Y-H. Anal. Methods. 2014b; 6:4152–4157.

Loan PTK, Zhang W, Lin C-T, Wei K-H, Li L-J, Chen C-H. Adv. Mater. 2014; 26:4838–4844. [PubMed: 24841824]

Loo AH, Bonanni A, Ambrosi A, Pumera M. Nanoscale. 2014; 6:11971–11975. [PubMed: 25177907]

Lubin AA, Plaxco KW. Acc. Chem. Res. 2010; 43:496–505. [PubMed: 20201486]

Ma R, Liu Z, Li L, Iyi N, Sasaki T. J. Mater. Chem. 2006; 16:3809–3813.

Ma R, Sasaki T. Adv. Mater. 2010; 22:5082–5104. [PubMed: 20925100]

Mao K, Wu Z, Chen Y, Zhou X, Shen A, Hu J. Talanta. 2015; 132:658–663. [PubMed: 25476360]

McCarthy JJ, Hilfiker R. Nat. Biotechnol. 2000; 18:505–508. [PubMed: 10802616]

McLaren A, Valdes-Solis T, Li G, Tsang SC. J. Am. Chem. Soc. 2009; 131:12540–12541. [PubMed: 19685892]

Meng F, Li J, Cushing SK, Zhi M, Wu N. J. Am. Chem. Soc. 2013; 135:10286–10289. [PubMed: 23808935]

Miyake Y, Togashi H, Tashiro M, Yamaguchi H, Oda S, Kudo M, Tanaka Y, Kondo Y, Sawa R, Fujimoto T, Machinami T, Ono A. J. Am. Chem. Soc. 2006; 128:2172–2173. [PubMed: 16478145]

Moses PG, Mortensen JJ, Lundqvist BI, Norskov JK. J. Chem. Phys. 2009; 130:104709. [PubMed: 19292551]

Osada M, Ebina Y, Takada K, Sasaki T. Adv. Mater. 2006; 18:295–299.

Osada M, Itose M, Ebina Y, Ono K, Ueda S, Kobayashi K, Sasaki T. Appl. Phys. Lett. 2008; 92:253110.

Osada M, Sasaki T. J. Mater. Chem. 2009; 19:2503–2511.

Osada M, Sasaki T. Adv. Mater. 2012; 24:210–228. [PubMed: 21997712]

Osada M, Sasaki T. Polymer Journal. 2015; 47:89–98.

Osborne SE, Matsumura I, Ellington AD. Curr. Opin. Chem. Biol. 1997; 1:5–9. [PubMed: 9667829]

Pumera M, Loo AH. Trac-Trend. Anal. Chem. 2014; 61:49–53.

Qin Y, Ma Y, Jin X, Zhang L, Ye G, Zhao S. Anal. Chim. Acta. 2015; 866:84–89. [PubMed: 25732696]

Radisavljevic B, Radenovic A, Brivio J, Giacometti V, Kis A. Nat. Nanotechnol. 2011a; 6:147–150. [PubMed: 21278752]

Radisavljevic B, Whitwick MB, Kis A. ACS Nano. 2011b; 5:9934–9938. [PubMed: 22073905]

Rao CNR, Matte HSSR, Maitra U. Angew. Chem. Int. Ed. 2013; 52:13162–13185.

Rurack K. Spectrochim. Acta A. 2001; 57:2161–2195.

Sakai N, Ebina Y, Takada K, Sasaki T. J. Phys. Chem. B. 2005; 109:9651–9655. [PubMed: 16852162]

Sarkar D, Xie X, Kang J, Zhang H, Liu W, Navarrete J, Moskovits M, Banerjee K. Nano Lett. 2015; 15:2852–2862. [PubMed: 25723363]

Sasaki T. J. Ceram. Soc. Jpn. 2007; 115:9–16.

Schwierz F. Nat. Nanotechnol. 2011; 6:135–136. [PubMed: 21372836]

Shibata T, Sakai N, Fukuda K, Ebina Y, Sasaki T. Phys. Chem. Chem. Phys. 2007; 9:2413–2420. [PubMed: 17492105]

Shukoor MI, Altman MO, Han D, Bayrac AT, Ocsoy I, Zhu Z, Tan W. ACS Appl. Mater. Interfaces. 2012; 4:3007–3011. [PubMed: 22650355]

Su S, Chao J, Pan D, Wang L, Fan C. Electroanalysis. 2015; 27:1062–1072.

Sun G, Liu J, Zhang X, Wang X, Li H, Yu Y, Huang W, Zhang H, Chen P. Angew. Chem. Int. Ed. 2014a; 53:12576–12580.

Sun Y, Gao S, Xie Y. Chem. Soc. Rev. 2014b; 43:530–546. [PubMed: 24122032]

Tan C, Yu P, Hu Y, Chen J, Huang Y, Cai Y, Luo Z, Li B, Lu Q, Wang L, Liu Z, Zhang H. J. Am. Chem. Soc. 2015; 137:10430–10436. [PubMed: 26241063]

Tan W, Donovan MJ, Jiang J. Chem. Rev. 2013; 113:2842–2862. [PubMed: 23509854]

Tan X, Chen W, Lu S, Zhu Z, Chen T, Zhu G, You M, Tan W. Anal. Chem. 2012; 84:8272–8276. [PubMed: 22916953]

Tan Y, Guo Q, Zhao X, Yang X, Wang K, Huang J, Zhou Y. Biosens. Bioelectron. 2014; 51:255–260. [PubMed: 23973935]

Tanaka K, Yamada Y, Shionoya M. J. Am. Chem. Soc. 2002; 124:8802–8803. [PubMed: 12137526]

Tang L, Wang Y, Li J. Chem. Soc. Rev. 2015; 44:6954–6980. [PubMed: 26144837]

Tang Z, Wu H, Cort JR, Buchko GW, Zhang Y, Shao Y, Aksay IA, Liu J, Lin Y. Small. 2010; 6:1205–1209. [PubMed: 20461727]

Tortolini C, Bollella P, Antonelli ML, Antiochia R, Mazzei F, Favero G. Biosens. Bioelectron. 2015; 67:524–531. [PubMed: 25263314]

Tuerk C, Gold L. Science. 1990; 249:505–510. [PubMed: 2200121]

Tyrakowski CM, Snee PT. Anal. Chem. 2014; 86:2380–2386. [PubMed: 24506832]

Velusamy V, Arshak K, Korostynska O, Oliwa K, Adley C. Biotechnol. Adv. 2010; 28:232–254. [PubMed: 20006978]

Voiry D, Yamaguchi H, Li J, Silva R, Alves DCB, Fujita T, Chen M, Asefa T, Shenoy VB, Eda G, Chhowalla M. Nat. Mater. 2013; 12:850–855. [PubMed: 23832127]

Wagenknecht HA. Angew. Chem. Int. Ed. 2003; 42:3204–3206.

Wang C, Zhai W, Wang Y, Yu P, Mao L. Analyst. 2015a; 140:4021–4029. [PubMed: 25919222]

Wang G, Wang Y, Chen L, Choo J. Biosens. Bioelectron. 2010; 25:1859–1868. [PubMed: 20129770]

Wang H, Yang R, Yang L, Tan W. ACS Nano. 2009; 3:2451–2460. [PubMed: 19658387]

Wang L, Sasaki T. Chem. Rev. 2014; 114:9455–9486. [PubMed: 24754464]

Wang Q, Zheng H, Gao X, Lin Z, Chen G. Chem. Commun. 2013; 49:11418–11420.

Wang QH, Kalantar-Zadeh K, Kis A, Coleman JN, Strano MS. Nat. Nanotechnol. 2012; 7:699–712. [PubMed: 23132225]

Wang S, Zhang Y, Ning Y, Zhang G-J. Analyst. 2015b; 140:434–439. [PubMed: 25426801]

Wang X, Nan F, Zhao J, Yang T, Ge T, Jiao K. Biosens. Bioelectron. 2015c; 64:386–391. [PubMed: 25262063]

Wang Y, Zhuang Q, Ni Y. J. Electroanal. Chem. 2015d; 736:47–54.

Wu W, Wang L, Li Y, Zhang F, Lin L, Niu S, Chenet D, Zhang X, Hao Y, Heinz TF, Hone J, Wang ZL. Nature. 2014; 514:470–474. [PubMed: 25317560]

Xi Q, Zhou D-M, Kan Y-Y, Ge J, Wu Z-K, Yu R-Q, Jiang J-H. Anal. Chem. 2014; 86:1361–1365. [PubMed: 24446758]

Xiang X, Shi J, Huang F, Zheng M, Deng Q, Xu J. Biosens. Bioelectron. 2015; 74:227–232. [PubMed: 26143463]

Xie J, Zhang J, Li S, Grote F, Zhang X, Zhang H, Wang R, Lei Y, Pan B, Xie Y. J. Am. Chem. Soc. 2013; 135:17881–17888. [PubMed: 24191645]

Xu M, Liang T, Shi M, Chen H. Chem. Rev. 2013; 113:3766–3798. [PubMed: 23286380]

Yang J, Voiry D, Ahn SJ, Kang D, Kim AY, Chhowalla M, Shin HS. Angew. Chem. Int. Ed. 2013; 52:13751–13754.

Yang K, Zeng M, Hu X, Guo B, Zhou J. Analyst. 2014a; 139:4445–4448. [PubMed: 25057513]

Yang W, Ratinac KR, Ringer SP, Thordarson P, Gooding JJ, Braet F. Angew. Chem. Int. Ed. 2010; 49:2114–2138.

Yang Y, Li C, Yin L, Liu M, Wang Z, Shu Y, Li G. ACS Appl. Mater. Interfaces. 2014b; 6:7579–7584. [PubMed: 24734899]

Yasun E, Gulbakan B, Ocsoy I, Yuan Q, Shukoor MI, Li C, Tan W. Anal. Chem. 2012; 84:6008–6015. [PubMed: 22725611]

Yin X, Cai J, Feng H, Wu Z, Zou J, Cai Q. New J. Chem. 2015; 39:1892–1898.

Yin Z, Li H, Li H, Jiang L, Shi Y, Sun Y, Lu G, Zhang Q, Chen X, Zhang H. ACS Nano. 2012; 6:74–80. [PubMed: 22165908]

Yoffe AD. Solid State Ionics. 1990; 39:1–7.

Yuan Y, Li R, Liu Z. Anal. Chem. 2014a; 86:3610–3615. [PubMed: 24611524]

Yuan Y, Wu S, Shu F, Liu Z. Chem. Commun. 2014b; 50:1095–1097.

Zhang Y, Zheng B, Zhu C, Zhang X, Tan C, Li H, Chen B, Yang J, Chen J, Huang Y, Wang L, Zhang H. Adv. Mater. 2015; 27:935–939. [PubMed: 25504749]

Zhao J, Jin X, Vdovenko M, Zhang L, Sakharov IY, Zhao S. Chem. Commun. 2015a; 51:11092–11095.

Zhao J, Ma Y, Kong R, Zhang L, Yang W, Zhao S. Anal. Chim. Acta. 2015b; 887:216–223. [PubMed: 26320805]

Zhao Y, Chen F, Li Q, Wang L, Fan C. Chem. Rev. 2015c; 115:12491–12545. [PubMed: 26551336]

Zhao Z, Fan H, Zhou G, Bai H, Liang H, Wang R, Zhang X, Tan W. J. Am. Chem. Soc. 2014; 136:11220–11223. [PubMed: 25061849]

Zheng J, Yang RH, Shi ML, Wu CC, Fang XH, Li YH, Li JH, Tan WH. Chem. Soc. Rev. 2015; 44:3036–3055. [PubMed: 25777303]

Zhou P, Luo Q, Lin Y, Chen L, Li S, Zhou G, Ji X, He Z. Anal. Chem. 2012; 84:7343–7349. [PubMed: 22888831]

Zhu C, Zeng Z, Li H, Li F, Fan C, Zhang H. J. Am. Chem. Soc. 2013; 135:5998–6001. [PubMed: 23570230]

Zhu CZ, Dan D, Lin YH. 2D Mater. 2015; 2:032004.

Highlights

- A summary of recent progress in nucleic acid-functionalized transition metal nanosheets for biosensing applications are presented.
- The combination of 2D transition metal nanomaterials and nucleic acids brings intriguing opportunities in bioanalysis and biomedicine.
- The applications in the context of different signal transducing mechanisms, including optical and electrochemical approaches are introduced.
- The perspectives on the current challenges and opportunities in this promising field are also discussed.

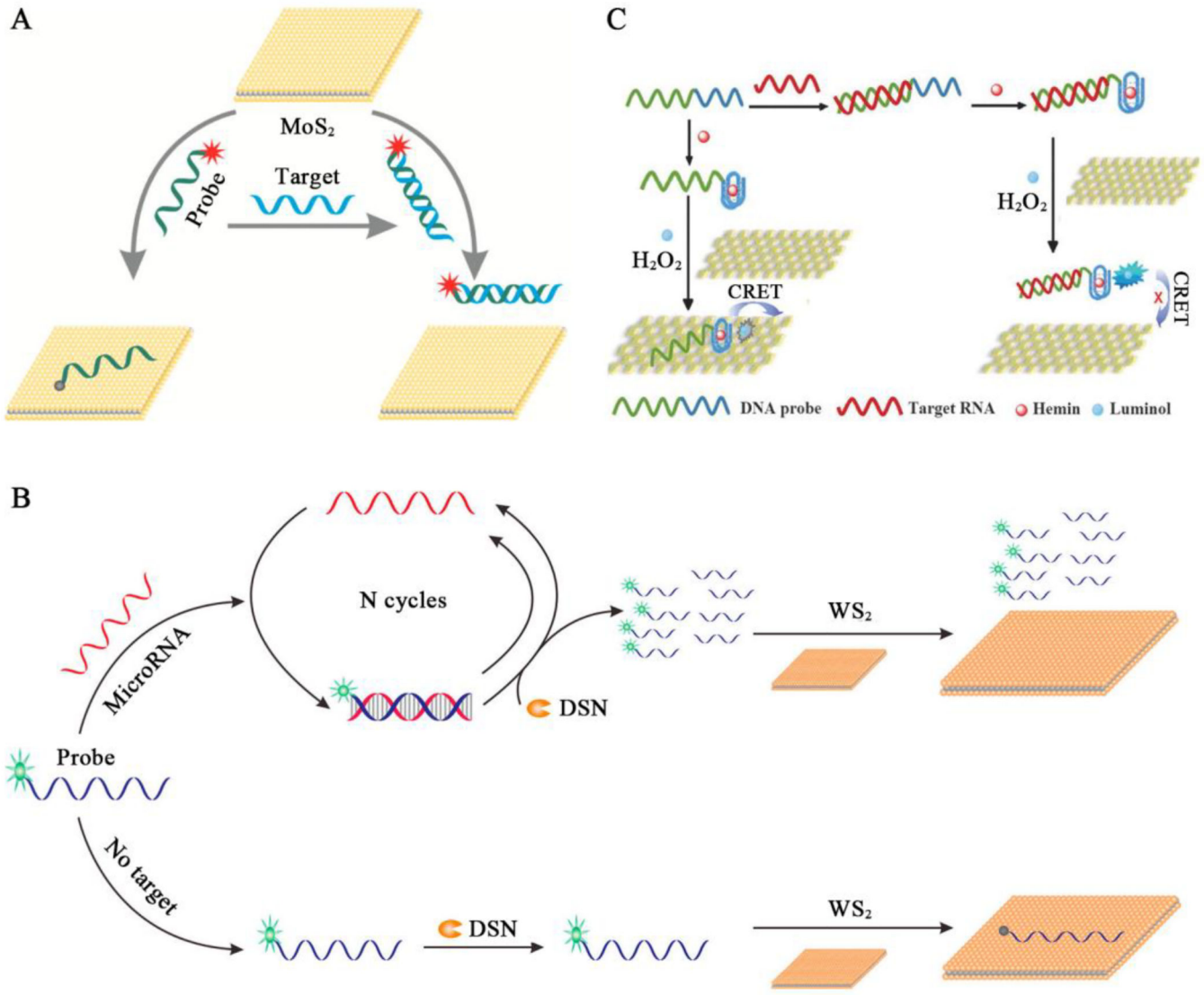

Fig. 1.

Optical biosensors for nucleic acid detection based on nucleic acid-functionalized transition metal nanosheets. (A) Schematic illustration of the fluorimetric DNA assay based on MoS_2 nanosheets as biosensors. Reproduced with permission from Zhu et al. (2013). Copyright 2013 American Chemical Society. (B) Schematic illustration of the miRNA assay based on WS_2 nanosheet-mediated fluorescence quenching and duplex-specific nuclease signal amplification. Reproduced with permission from Xi et al. (2014). Copyright 2014 American Chemical Society. (C) Schematic illustration of the WS_2 nanosheet-based CRET platform for DNA detection. Reproduced with permission from Zhao et al. (2015a). Copyright 2015 Royal Society of Chemistry.

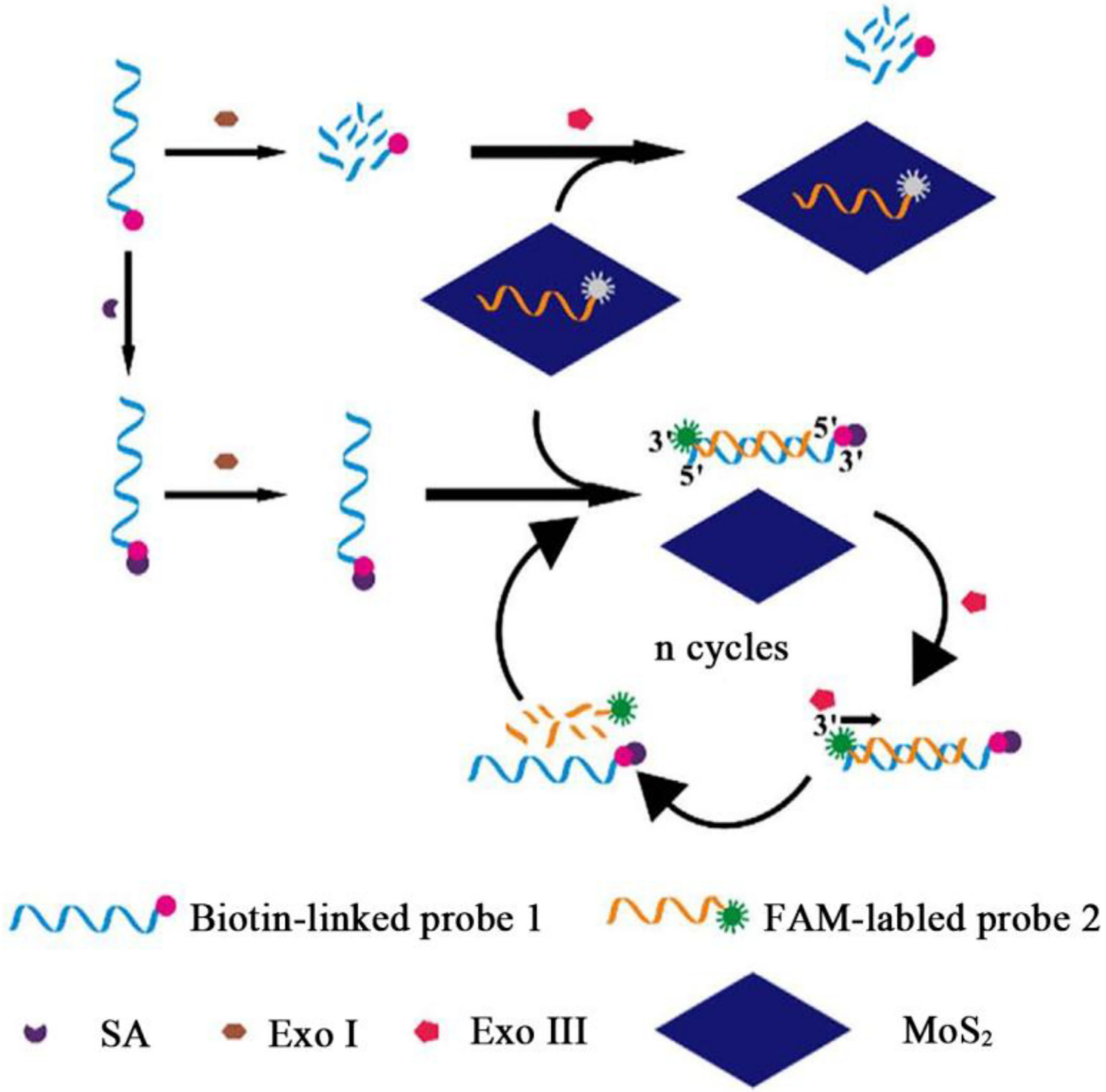

Fig. 2.

Schematic illustration of the mechanism of a MoS_2-based biosensor for SA detection via TPSMLD. Reproduced with permission from Xiang et al. (2015). Copyright 2015 Elsevier.

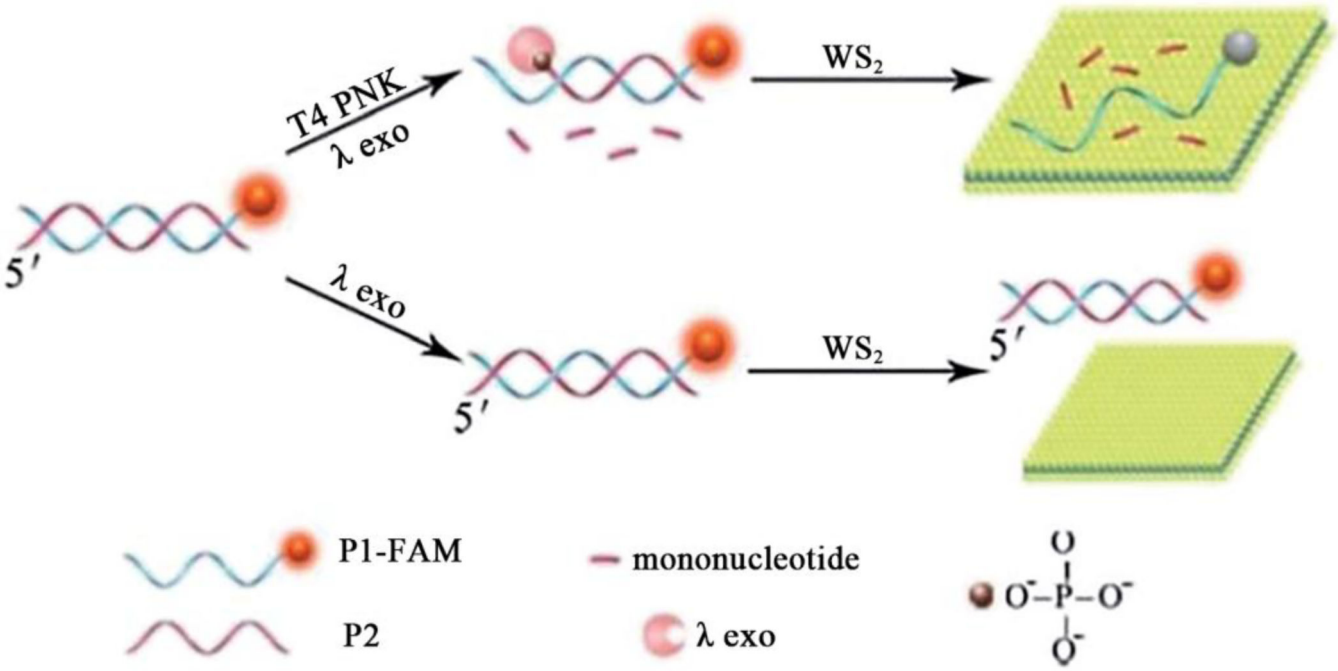

Fig. 3.

Schematic illustration of the WS_2 nanosheet-based platform for analysis of T4 PNK activity and inhibition. Reproduced with permission from Ge et al. (2014b). Copyright 2014 Royal Society of Chemistry.

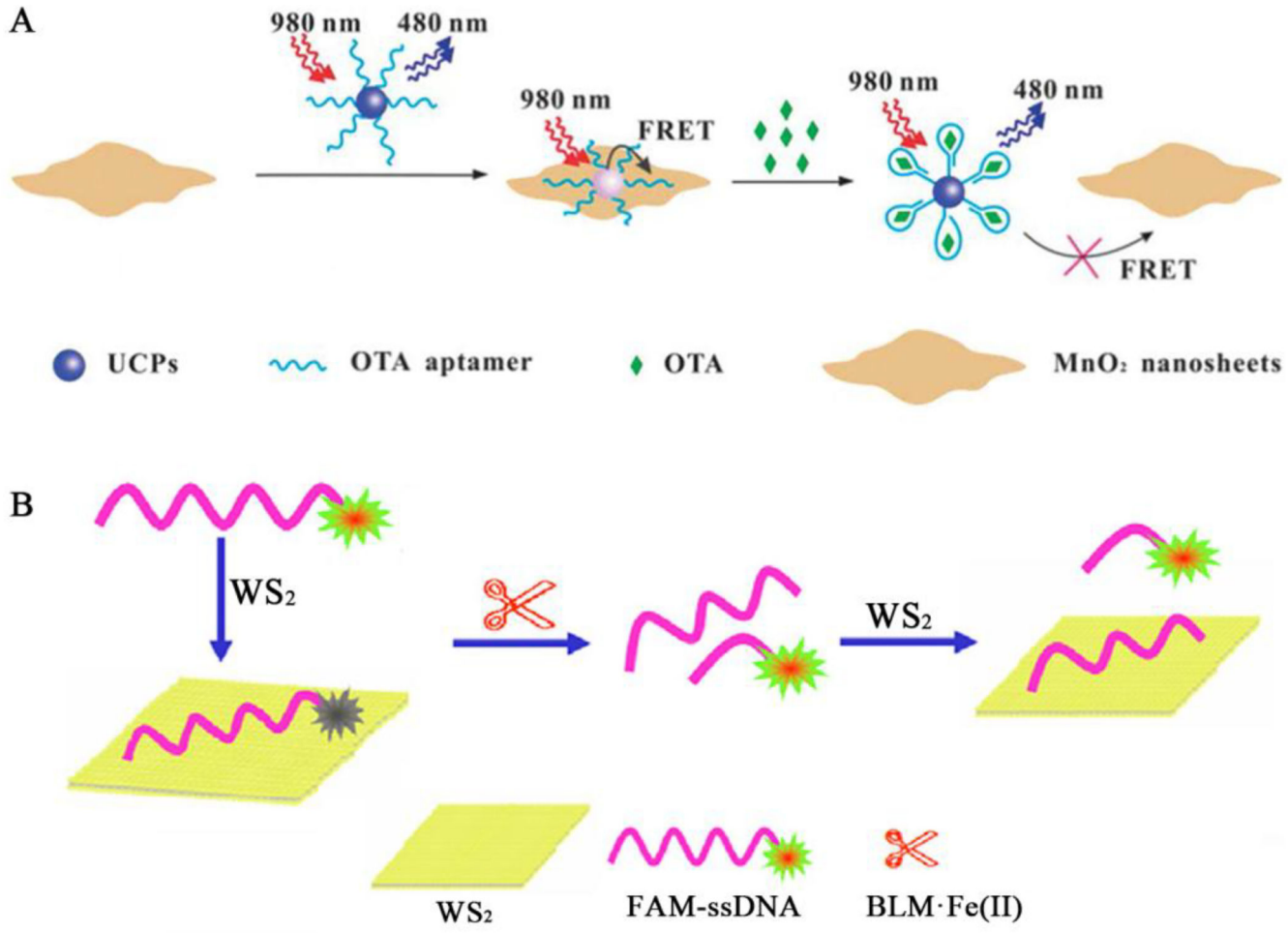

Fig. 4.

Optical biosensors for organic small-molecule detection based on nucleic acid-functionalized transition metal nanosheets. Reproduced with permission from Yuan et al. (2014b). Copyright 2013, Royal Society of Chemistry. (A) Schematic illustration of MnO_2 nanosheet-based FRET aptasensing. (B) Schematic illustration of WS_2 nanosheet-based fluorescence strategy for bleomycin detection. Reproduced with permission from Qin et al. (2015). Copyright 2015 Elsevier.

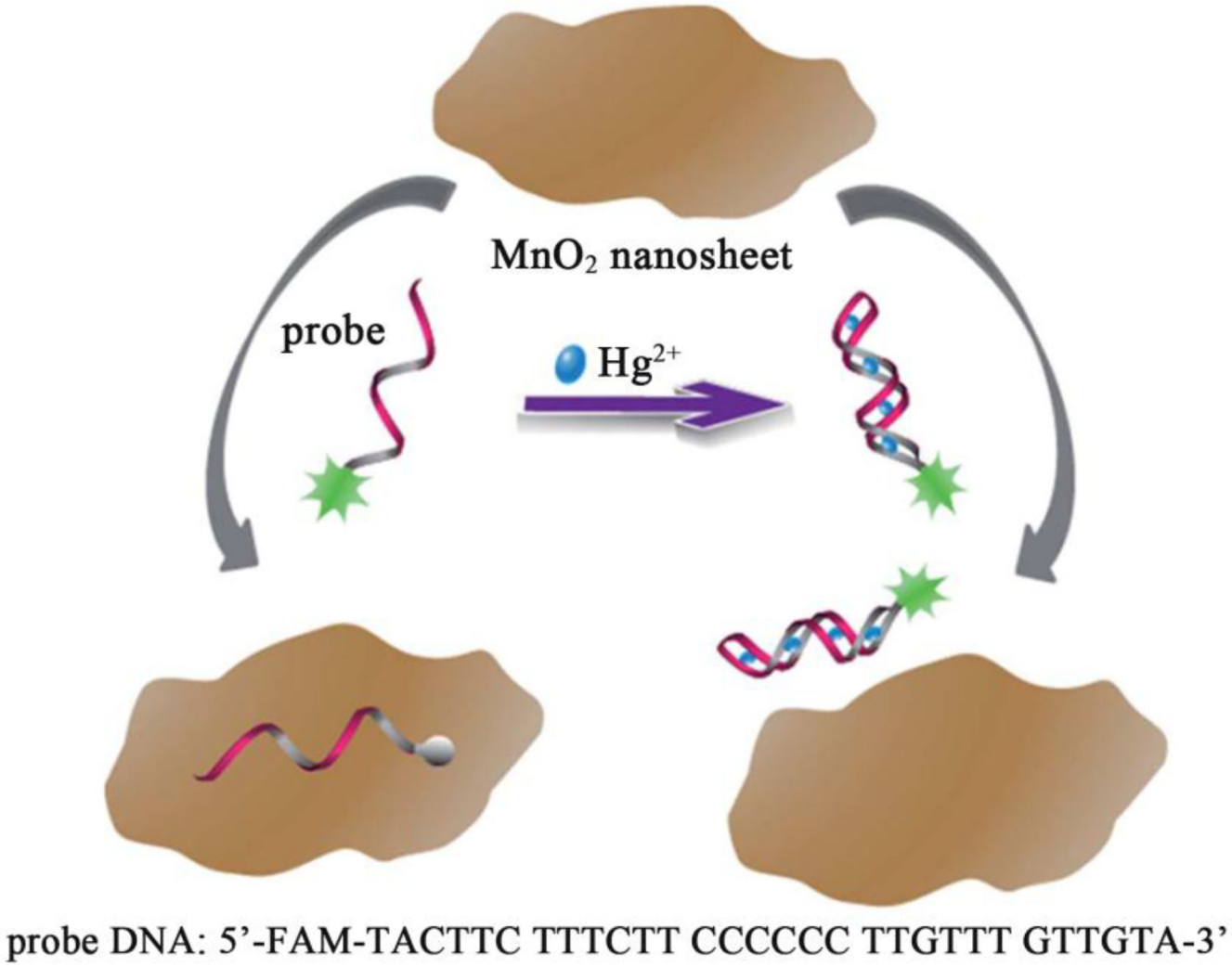

Fig. 5.

Schematic illustration of the fluorescence sensor for Hg^{2+} based on MnO_2 nanosheet. Reproduced with permission from Yang et al. (2014a). Copyright 2014 Royal Society of Chemistry.

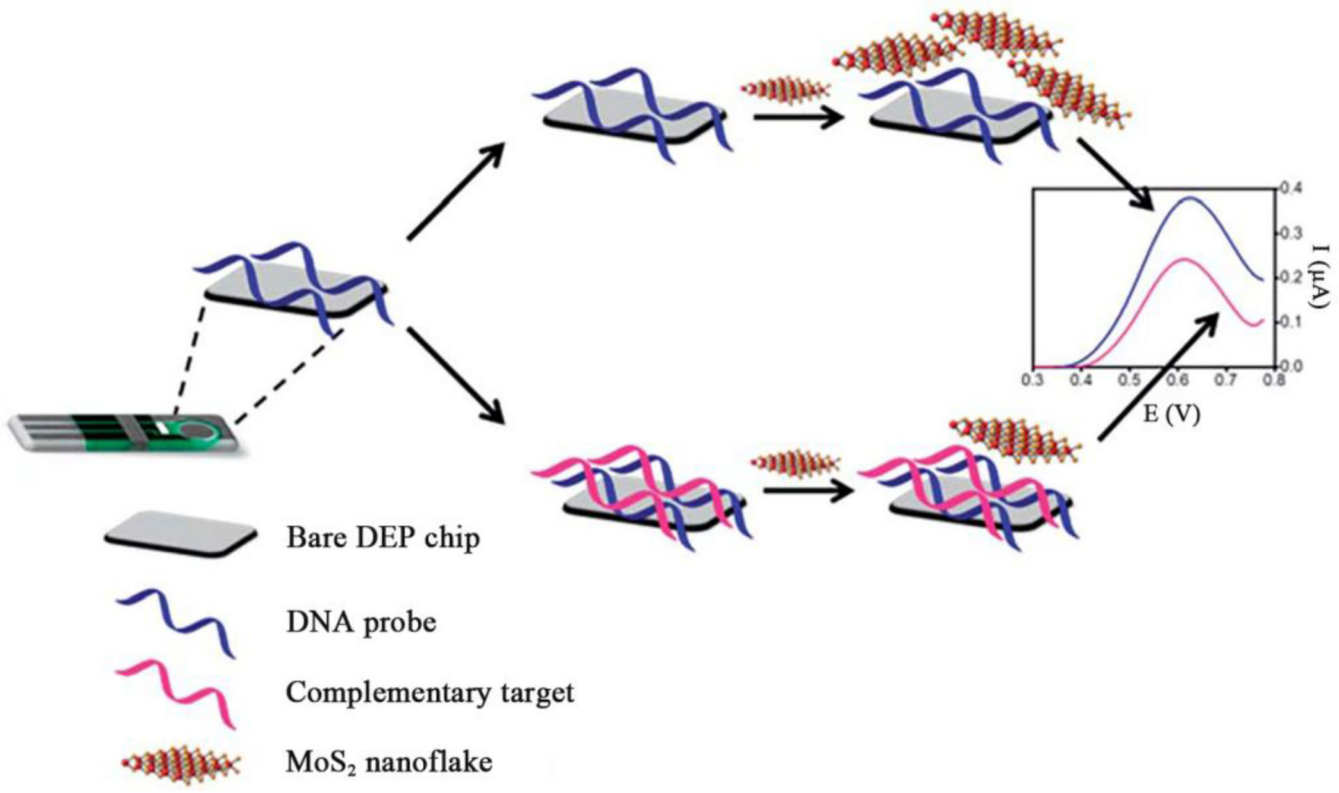

Fig. 6.

Schematic illustration of the DNA assay based on MoS_2 nanosheets as inherently electroactive labels. Reproduced with permission from Loo et al. (2014). Copyright 2014 Royal Society of Chemistry.

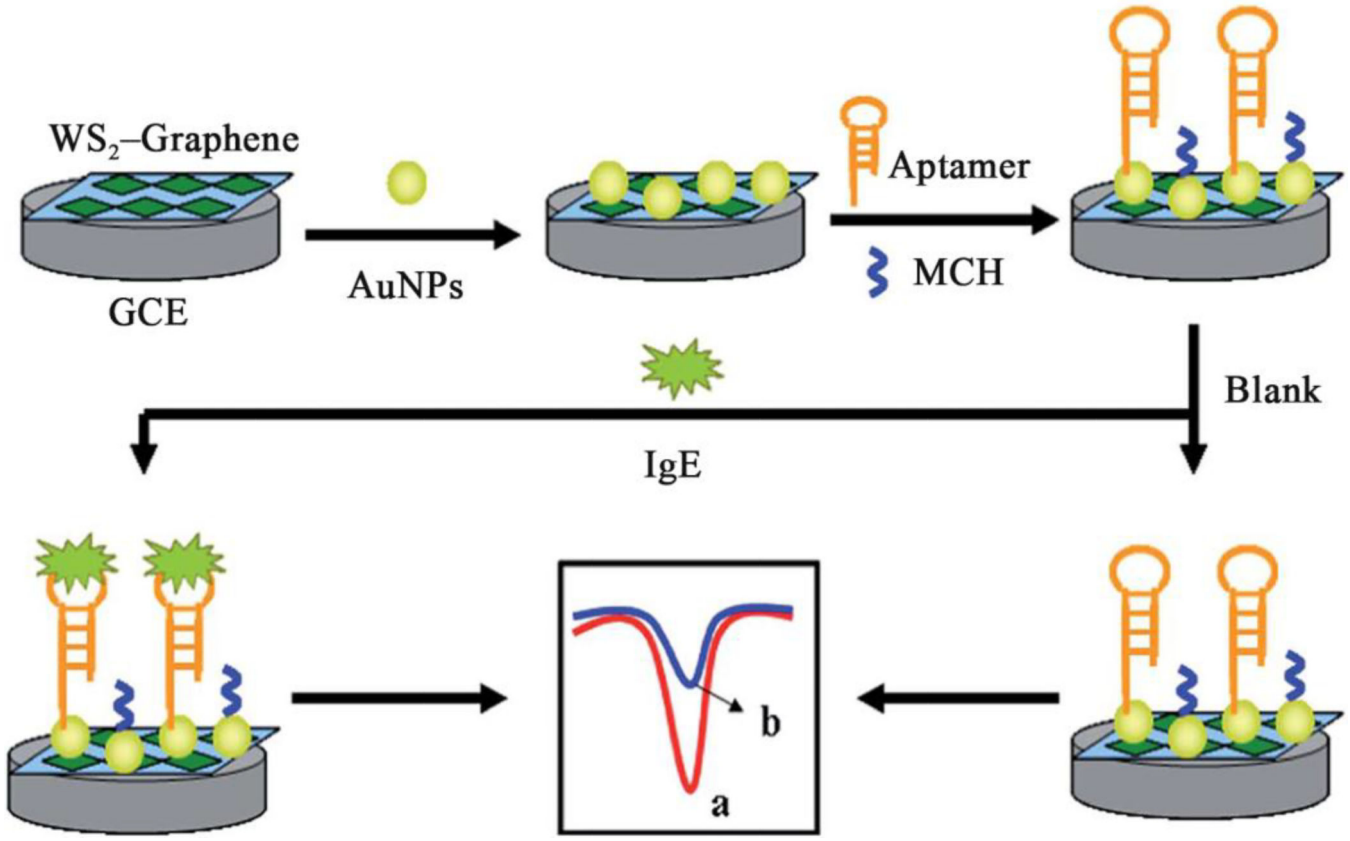

Fig. 7.

Schematic illustration of the IgE aptasensor based on WS_2-graphene nanosheets and AuNPs. Reproduced with permission from Huang et al. (2014a). Copyright 2014 Royal Society of Chemistry.

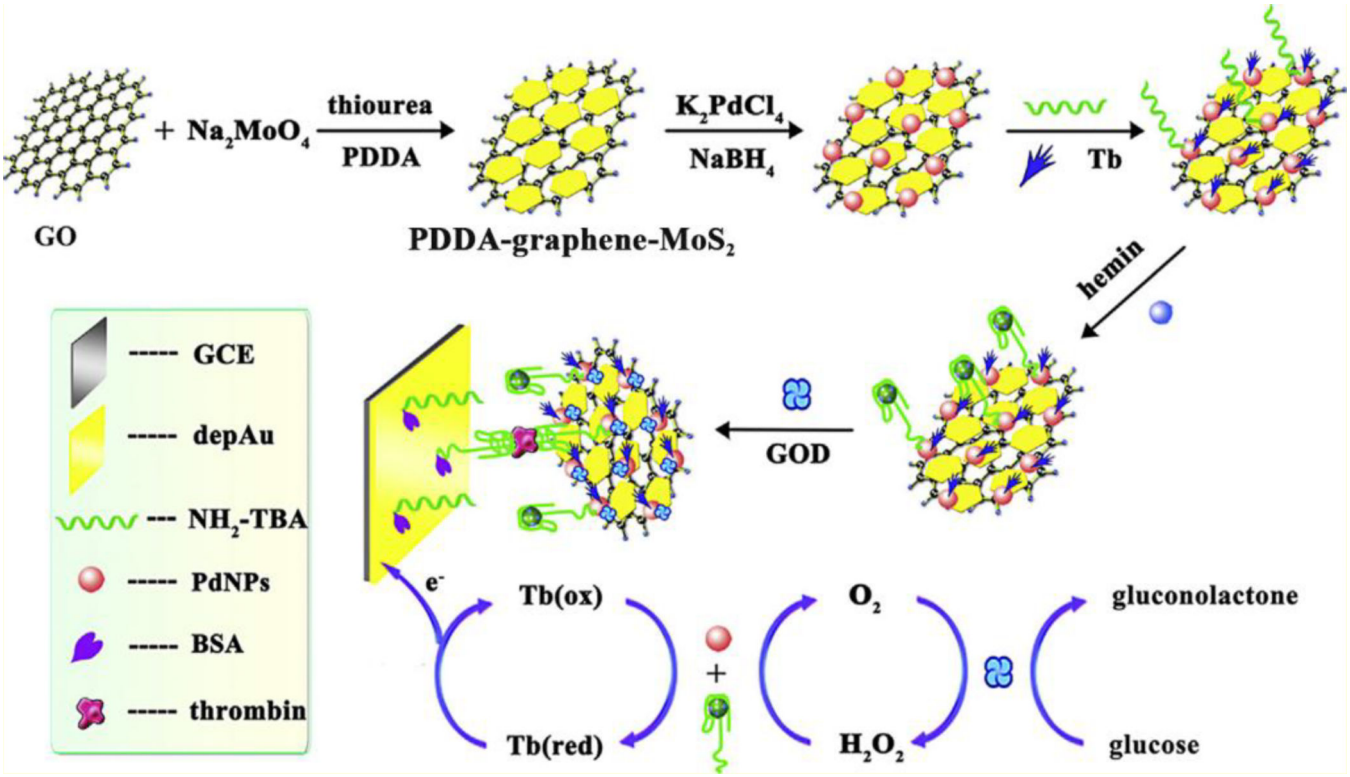

Fig. 8.

Schematic illustration of the thrombin aptasensor based on PdNPs/PDDA-graphene-MoS_2 flower-like nanocomposites and enzymatic signal amplification. Reproduced with permission from Jing et al. (2015). Copyright 2014 Elsevier.

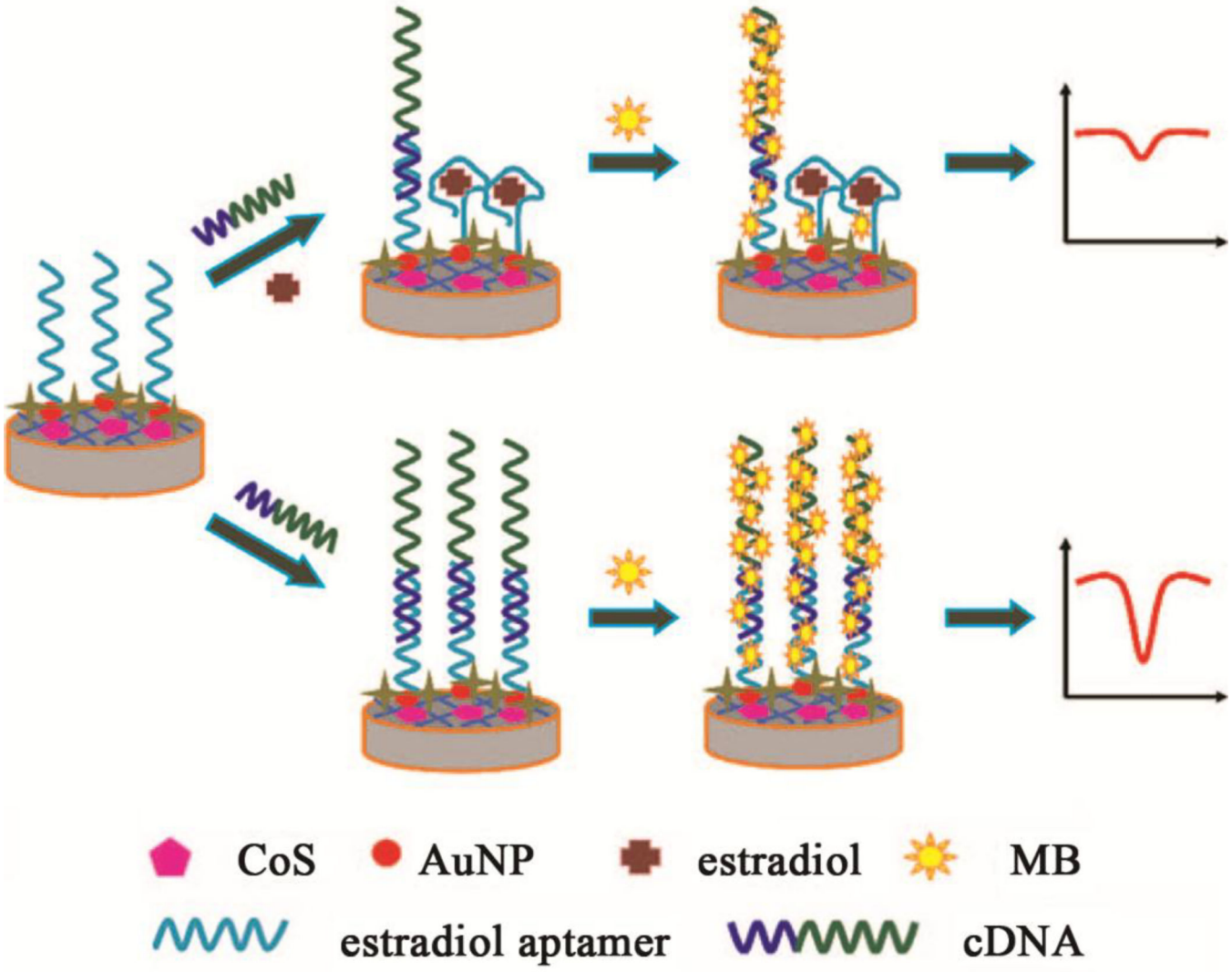

Fig. 9.

Schematic illustration of the electrochemical aptasensor for 17β-estradiol detection. Reproduced with permission from Huang et al. (2015c). Copyright 2014 Elsevier.